Dynamic cylindrical shell equations by power series expansions

Dynamic cylindrical shell equations by power series expansions

A.M. Hägglund, P.D. Folkow *,

Department of Applied Mechanics, Chalmers University of Technology, SE-412 96 Göteborg, Sweden

Abstract

The dynamics of an infinite circular cylindrical shell is considered. The derivation process is based on power series expansions of the displacement components in the radial direction. By using these expansions in the three dimensional equations of motions, a set of recursion relations is identified expressing higher displacement coefficients in terms of lower order ones. The new approximate shell equations are hereby obtained from the boundary conditions, resulting in a set of six partial differential equations. These equations are believed to be asymptotically correct and it is, in principle, possible to go to any order. Equations of order up to and including the square of the thickness h^2 are presented explicitly. This set of six equations are reduced to five as well as three equations and compared to classical theories. Dispersion curves, together with the eigenfrequencies for a 2D case, are calculated using exact, classical and expansion theories. It is shown that the approximate equations containing order h^2 are in general as good as or better than the established theory of the same order.

Key words: cylindrical shell, ring, power series, asymptotic, dispersion curves

1 Introduction

A shell may be regarded as a curved plate, where the thickness is small compared to the shell's other geometrical dimensions as well as to the wavelengths of importance. Shells are common in many structural systems, such as pressure vessels, ship hulls, airplanes and car bodies. The main reason for this

* Corresponding author. Tel: +46 31 7721521, Fax: +46 31 772 3827.
Email address: peter.folkow@chalmers.se (P.D. Folkow).

is that shell structures exhibit low weight and high strength thanks to their membrane stiffness; an effect not exploited in most plate structures.

The investigation of the governing equations for cylindrical shells has been of great interest in the history of elastodynamic theory, ranging from the exact three-dimensional theory to simplified approximate theories. The three-dimensional theory has been studied by several authors (Gazis, 1958; Armenakas et al., 1969), but the bulk of analysis has been on various approximate models due to the complexity of the exact theory. In these simplified theories, both the dynamic equations and the boundary conditions are often derived using various kinds of simplifying kinematic assumptions. There is much debate on the correctness of these assumptions, and as the engineering demands increase continuously, resulting in more complex shell structures and the need for higher computational accuracies, it becomes more crucial to choose the most appropriate simplifications. This calls for a systematic approach when tackling the dynamic behavior of the shell structures in question, which is the main purpose of the present paper.

The simplest shell theory of practical use is the membrane theory (Graff, 1975), where the transverse force and the bending moment are assumed negligibly small. The next level is to include both transverse forces and bending moments, but neglect shear deformation and rotary inertia. In this case there are numerous different theories, which makes the situation somewhat different from beams and plates. The classical bending theory is due to Love (Graff, 1975), and this model has been further developed by others (Naghdi and Berry, 1954; Sanders, 1959). By including shear deformation and rotary inertia, more involved equations are obtained. As for the bending theories there are several different models that have been proposed, e.g. (Naghdi and Cooper, 1956; Mirsky and Herrmann, 1957; Soedel, 1982). These models involve shear correction factors, in line with Timoshenko's beam theory and Mindlin's plate theory.

Several different approaches exist that use series expansion techniques for cylindrical shells. Kennard (1953) has developed a model based on power series expansions of the stresses and displacements. This rather complicated derivation leads to a set of equations of motion that was dismissed by Naghdi (1956) as being "meaningless" due to lack of consistency. Other more or less systematic series expansion approaches have been presented ever since, (McNiven et al., 1966; Johnson and Widera, 1969; Faraji and Archer, 1985; Gardner, 1985; Hirano and Hirashima, 1989; McDaniel and Ginsberg, 1993; Niordson, 2000). Although quite different in the derivation process, these theories all have in common that artificial assumptions are taken to a minimum, including terms such as shear correction factors.

A comprehensive survey regarding different cylindrical shell theories is given

by Leissa (1973), while a more recent review of papers on dynamic shell structures is given by Qatu (2002).

In this paper, the attention is on the derivation of the governing dynamic equations for an infinite, unloaded, linearly elastic, isotropic, cylindrical shell. The method used is based on a series expansion technique which is different from the ones discussed above. Here, the displacement fields are expanded using power series in the thickness coordinate. This is accomplished in a systematic manner up to an (in principle) arbitrary order. There are good reasons to believe that the approach leads to asymptotically correct equations, without using *ad hoc* assumptions. The analytical form of the equations are compared to classical theories and dispersion curves as well as the lowest eigenfrequencies in the 2D case of plane strain are given for exact, classical and expansion theories.

The present method has previously been adopted for rods (Boström, 2000), plates (Boström et al., 2001), and for piezoelectric layers (Johansson and Niklasson, 2003; Mauritsson et al., 2008). It should be noted that the somewhat different approach that was used by Johansson and Folkow (2007) and Johansson et al. (2005) on fluid-loaded elastic and porous plates, actually renders the same results as the present method.

2 Power series expansions

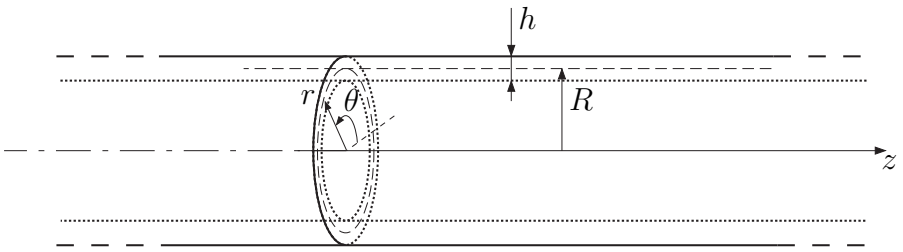

Fig. 1. An infinite circular cylindrical shell.

Consider a circular cylindrical shell with middle surface radius R and thickness h, illustrated in Figure 1. The shell is homogeneous, isotropic and linearly elastic with density ρ and Lamé constants λ and μ. Cylindrical coordinates are used with radial coordinate r, circumferential coordinate θ and axial coordinate z. Along the axis of revolution of the cylinder, coinciding with the coordinate axis z, the cylinder is infinite. The corresponding displacement fields are denoted u, v and w. Adopting the three-dimensional equations of

motion gives

$$\begin{aligned}
&\frac{\partial \sigma_{rr}}{\partial r}+\frac{1}{r}\frac{\partial \sigma_{r\theta}}{\partial \theta}+\frac{\partial \sigma_{rz}}{\partial z}+\frac{\sigma_{rr}-\sigma_{\theta\theta}}{r}=\rho\frac{\partial^2 u}{\partial t^2},\\
&\frac{1}{r}\frac{\partial \sigma_{\theta\theta}}{\partial \theta}+\frac{\partial \sigma_{r\theta}}{\partial r}+\frac{\partial \sigma_{\theta z}}{\partial z}+2\frac{\sigma_{r\theta}}{r}=\rho\frac{\partial^2 v}{\partial t^2},\\
&\frac{\partial \sigma_{zz}}{\partial z}+\frac{\partial \sigma_{rz}}{\partial r}+\frac{1}{r}\frac{\partial \sigma_{\theta z}}{\partial \theta}+\frac{\sigma_{rz}}{r}=\rho\frac{\partial^2 w}{\partial t^2}.
\end{aligned} \tag{1}$$

The stresses may be expressed in terms of the displacement fields according to

$$\sigma_{rr}=\lambda\left[\frac{1}{r}\frac{\partial}{\partial r}(ru)+\frac{1}{r}\frac{\partial v}{\partial \theta}+\frac{\partial w}{\partial r}\right]+2\mu\frac{\partial u}{\partial r}, \tag{2a}$$

$$\sigma_{\theta\theta}=\lambda\left[\frac{1}{r}\frac{\partial}{\partial r}(ru)+\frac{1}{r}\frac{\partial v}{\partial \theta}+\frac{\partial w}{\partial r}\right]+2\mu\left[\frac{u}{r}+\frac{1}{r}\frac{\partial v}{\partial \theta}\right], \tag{2b}$$

$$\sigma_{zz}=\lambda\left[\frac{1}{r}\frac{\partial}{\partial r}(ru)+\frac{1}{r}\frac{\partial v}{\partial \theta}+\frac{\partial w}{\partial r}\right]+2\mu\frac{\partial w}{\partial z}, \tag{2c}$$

$$\sigma_{r\theta}=\mu\left[\frac{1}{r}\frac{\partial u}{\partial \theta}+\frac{\partial v}{\partial r}-\frac{v}{r}\right], \tag{2d}$$

$$\sigma_{rz}=\mu\left[\frac{\partial u}{\partial z}+\frac{\partial w}{\partial r}\right], \tag{2e}$$

$$\sigma_{\theta z}=\mu\left[\frac{\partial v}{\partial z}+\frac{1}{r}\frac{\partial w}{\partial \theta}\right]. \tag{2f}$$

Introduce $r=R+\xi$ where $-h/2\leq\xi\leq h/2$. To derive shell equations the displacement components are now expanded in power series in the thickness coordinate ξ (Boström, 2000; Boström et al., 2001; Johansson and Niklasson, 2003; Mauritsson et al., 2008)

$$\begin{aligned}
u&=u_0(z,\theta,t)+\xi u_1(z,\theta,t)+\xi^2 u_2(z,\theta,t)+\ldots,\\
v&=v_0(z,\theta,t)+\xi v_1(z,\theta,t)+\xi^2 v_2(z,\theta,t)+\ldots\\
w&=w_0(z,\theta,t)+\xi w_1(z,\theta,t)+\xi^2 w_2(z,\theta,t)+\ldots.
\end{aligned} \tag{3}$$

Note that these expansions involve both even and odd powers of ξ as symmetric and antisymmetric motions with respect to ξ do not decouple (Johansson and Niklasson, 2003; Mauritsson et al., 2008), contrary to the situation for rods and plates (Boström, 2000; Boström et al., 2001).

Insertion of the expansions (3) into the equations of motion (1) using (2a)–(2f)

and identifying equal powers of ξ yields the recursion formulas

$$
\begin{aligned}
u_{j+2} =& \frac{1}{R^2(j+1)(j+2)(\lambda+2\mu)} \\
&\Big[\rho\Big(\frac{\partial^2 u_{j-2}}{\partial t^2} + 2R\frac{\partial^2 u_{j-1}}{\partial t^2} + R^2\frac{\partial^2 u_j}{\partial t^2}\Big) \\
&-\mu\Big(\frac{\partial^2 u_{j-2}}{\partial z^2} + 2R\frac{\partial^2 u_{j-1}}{\partial z^2} + R^2\frac{\partial^2 u_j}{\partial z^2} + \frac{\partial^2 u_j}{\partial \theta^2}\Big) \\
&-(\lambda+2\mu)\Big((j^2-1)u_j + R(j+1)(2j+1)u_{j+1}\Big) \\
&-\Big((j-1)\lambda + (j-3)\mu\Big)\frac{\partial v_j}{\partial \theta} + R(j+1)(\lambda+\mu)\frac{\partial v_{j+1}}{\partial \theta} \\
&-(\lambda+\mu)\Big((j+1)\frac{\partial w_{j-1}}{\partial z} + 2Rj\frac{\partial w_j}{\partial z} + R^2(j+1)\frac{\partial w_{j+1}}{\partial z}\Big)\Big],
\end{aligned}
\tag{4a}
$$

$$
\begin{aligned}
v_{j+2} =& \frac{1}{R^2(j+1)(j+2)\mu} \\
&\Big[\rho\Big(\frac{\partial^2 v_{j-2}}{\partial t^2} + 2R\frac{\partial^2 v_{j-1}}{\partial t^2} + R^2\frac{\partial^2 v_j}{\partial t^2}\Big) \\
&-\mu\Big(\frac{\partial^2 v_{j-2}}{\partial z^2} + 2R\frac{\partial^2 v_{j-1}}{\partial z^2} + R^2\frac{\partial^2 v_j}{\partial z^2}\Big) + (\lambda+2\mu)\frac{\partial^2 v_j}{\partial \theta^2} \\
&-\mu\Big((j^2-1)v_j + R(j+1)(2j+1)v_{j+1}\Big) \\
&-\Big((j+1)\lambda + (j+3)\mu\Big)\frac{\partial u_j}{\partial \theta} + R(j+1)(\lambda+\mu)\frac{\partial u_{j+1}}{\partial \theta} \\
&-(\lambda+\mu)\Big(\frac{\partial^2 w_{j-1}}{\partial \theta \partial z} + R\frac{\partial^2 w_j}{\partial \theta \partial z}\Big)\Big],
\end{aligned}
\tag{4b}
$$

$$
\begin{aligned}
w_{j+2} =& \frac{1}{R^2(j+1)(j+2)\mu} \\
&\Big[\rho\Big(\frac{\partial^2 w_{j-2}}{\partial t^2} + 2R\frac{\partial^2 w_{j-1}}{\partial t^2} + R^2\frac{\partial^2 w_j}{\partial t^2}\Big) \\
&-(\lambda+2\mu)\Big(\frac{\partial^2 w_{j-2}}{\partial z^2} + 2R\frac{\partial^2 w_{j-1}}{\partial z^2} + R^2\frac{\partial^2 w_j}{\partial z^2}\Big) + \mu\frac{\partial^2 w_j}{\partial \theta^2} \\
&-\mu\Big(j^2 w_j + R(j+1)(2j+1)w_{j+1}\Big) \\
&-(\lambda+\mu)\Big(j\frac{\partial u_{j-1}}{\partial z} + R(2j+1)\frac{\partial u_j}{\partial z} + R^2(j+1)\frac{\partial u_{j+1}}{\partial z}\Big) \\
&-(\lambda+\mu)\Big(\frac{\partial^2 v_{j-1}}{\partial \theta \partial z} + R\frac{\partial^2 v_j}{\partial \theta \partial z}\Big)\Big],
\end{aligned}
\tag{4c}
$$

for $j = 0, 1, \ldots$. Here $u_j, v_j, w_j \equiv 0$ for $j < 0$. By using Eqs. (4) recursively all subsequent expressions involving u_j, v_j, w_j with $j = \{2, 3, \ldots\}$ may thus be written in terms of u_j, v_j, w_j with $j = \{0, 1\}$. These relations are no further approximations, they stem from the definition of the series expansions (3) and are as such exact.

From now on, the outer and inner ring surfaces are assumed free: $\sigma_{rr} = \sigma_{r\theta} =$

$\sigma_{rz} = 0$ for $\xi = \pm h/2$. It is convenient to express these boundary conditions in terms of the differences and sums of the surface stresses, as a common thickness factor (h) in the differences hereby can be cancelled out. This has the advantage of simplifying the numerical computations by reducing the contrast between large and small numbers. Introduce $\Delta\sigma = \sigma(h/2, \theta, t) - \sigma(-h/2, \theta, t)$ and $\Sigma\sigma = \sigma(h/2, \theta, t) + \sigma(-h/2, \theta, t)$ where σ is either σ_{rr}, $\sigma_{r\theta}$ or σ_{rz}. Hence, the six boundary conditions are

$$\begin{array}{lll} \Delta\sigma_{rr} = 0, & \Delta\sigma_{r\theta} = 0, & \Delta\sigma_{rz} = 0, \\ \Sigma\sigma_{rr} = 0, & \Sigma\sigma_{r\theta} = 0, & \Sigma\sigma_{rz} = 0. \end{array} \tag{5}$$

Using the series expansion (3) together with the recursion formulas (4) in the stress representations (2a), (2d) and (2e), it is straightforward to write the boundary conditions (5) in terms of the displacements u_j, v_j, w_j with $j = \{0, 1\}$. These partial differential equations are the sought new shell equations. When deriving the set of shell equations, the lengthy algebraic manipulations have been performed using the commercial code Mathematica [1] . The cases including h^4 and above would have been very difficult to derive without computer assisted algebra. In the derivation process, it is important to include terms of high enough power in the expansions Eq. (3) such that the resulting shell equations are consistent and stable for a given truncation level. Inspection reveals that it is enough to use expansions of order ξ^{j+1} to obtain correct truncated shell equations of order h^j. It is instructive to study how the recursion formulas effect the derivation process. Consider as an example the correctly truncated approximate shell equations up to and including h^2, which are obtained from using terms all up to u_3, v_3, w_3 in (3). Most other theories start from using fewer terms and end up with a set of equations of order h^2, see e.g. (Naghdi and Cooper, 1956; McNiven et al., 1966; Soedel, 1982; Gardner, 1985; Hirano and Hirashima, 1989). According to the present work these cited results are somehow inconsequent as the inclusion of the higher order terms would have produced extra h^2-terms. It is clear from this that the recursion formulas are crucial in order to avoid too many unknowns for a correct truncation.

Introducing the general matrix operator form $\mathcal{L}\vec{u} = \vec{0}$, the equation system becomes

$$\mathcal{L}_6\vec{u}_6 = \vec{0}, \tag{6}$$

where $\vec{u}_6 = (u_0, v_0, w_0, Ru_1, Rv_1, Rw_1)^T$. The six-by-six matrix operator $\mathcal{L}_6$ may be decomposed as

$$\mathcal{L}_6 = \mathcal{A}_6 + \eta\mathcal{B}_6 + \eta^2\mathcal{C}_6 + \ldots, \tag{7}$$

[1] Registered trademark of Wolfram Research Inc.

where $\eta = h^2/12R^2$ as only even powers in the thickness are present. Due to the way the boundary conditions are represented in $\mathcal{L}_6$, each matrix element involves either only odd spatial derivatives or only even spatial derivatives. The time derivatives are of even order throughout. When decomposing the operator $\mathcal{L}_6$ according to (7) the matrix corresponding to η^j involves derivatives up to order $2(j+1)$ in both space and time. Note that so far no approximations have been performed. Moreover, the expansion system is believed to be asymptotically correct (Boström, 2000; Boström et al., 2001; Johansson and Niklasson, 2003; Mauritsson et al., 2008; Johansson et al., 2005; Losin, 1997, 1998, 2001), see Section 4. The operator $\mathcal{L}_6$ may, in principle, be truncated to any order. However, the main interest here is to study lower order expansions as these are of most practical use. The explicit representation of $\mathcal{L}_6$ for the η^1 expansion is presented in Appendix A.

While it is convenient to work in terms of the field $\vec{u}_6$ when calculating the displacements (3) and the stresses (2) adopting (4), it is of some interest to further reduce the number of fields. In order to make comparisons with classical bending theories, only the three fields u_0, v_0 and w_0 are to be retained, while comparisons with theories involving shearing and rotary inertia are carried out using the five fields u_0, v_0, w_0, v_1, w_1, see Leissa (1973).

2.1 Shell equations in terms of u_0, v_0 and w_0

By applying differential operators to (6), it is straightforward to combine these equations in order to eliminate the fields u_1, v_1 and w_1. The new equation system becomes

$$\mathcal{L}_3\vec{u}_3 = \vec{0}, \tag{8}$$

where $\vec{u}_3 = (u_0, v_0, w_0)^T$ and $\mathcal{L}_3$ may be represented in line with Eq. (7). As in Eq. (6) no approximations have yet been performed. The elimination process is such that the truncated system in Eq. (6) results in a higher order system in (8). Specifically, the η^1 expansion in (6) causes terms all up to η^3 in (8). However, given a truncated η^j expansion in (6), only terms up to and including order η^j are believed to be asymptotically correct in (8) since these terms are unaltered when using a higher order system in (6). The truncated expansion in (6) is hereby not equivalent to the truncated set in (8) for a fixed order η^j.

The explicit representation of $\mathcal{A}_3$ is given as

$$\begin{aligned}
a_{11} &= 1 + \frac{\rho R^2\,(1-\nu^2)}{E}\frac{\partial^2}{\partial t^2}, \qquad a_{12} = a_{21} = \frac{\partial}{\partial \theta}, \qquad a_{13} = a_{31} = R\nu\frac{\partial}{\partial z}, \\
a_{22} &= \frac{\partial^2}{\partial \theta^2} + \frac{R^2(1-\nu)}{2}\frac{\partial^2}{\partial z^2} - \frac{\rho R^2\,(1-\nu^2)}{E}\frac{\partial^2}{\partial t^2}, \qquad a_{23} = a_{32} = \frac{R(1+\nu)}{2}\frac{\partial^2}{\partial \theta \partial z}, \\
a_{33} &= \frac{1-\nu}{2}\frac{\partial^2}{\partial \theta^2} + R^2\frac{\partial^2}{\partial z^2} - \frac{\rho R^2\,(1-\nu^2)}{E}\frac{\partial^2}{\partial t^2}.
\end{aligned} \tag{9}$$

Here, the Lamé constants are changed for Young's modulus E and Poisson's ratio ν to simplify comparisons to other theories. The equations are normalized so that a_{11}, a_{22} and a_{33} are in line with the bending theories given in (Leissa, 1973). The elements of $\mathcal{A}_3$ are seen to model the cylindrical membrane equations (Graff, 1975) as expected. The elements of $\mathcal{B}_3$ are not given explicitly here, as they involve the same sort of numerous higher order terms as $\mathcal{B}_6$, presented in Appendix A. It is noted that the elements of $\mathcal{A}_3$ and $\mathcal{B}_3$ are not that much altered when compared to $\mathcal{A}_6$ and $\mathcal{B}_6$. A comparison to classical theories that involve bending effects, such as the Love theory represented by $\mathcal{L}_L$, renders that $\mathcal{A}_L = \mathcal{A}_3$. Turning to the operator $\mathcal{B}_L$ it becomes (Graff, 1975; Leissa, 1973)

$$\begin{aligned}
b_{11} &= \frac{\partial^4}{\partial \theta^4} + 2R^2\frac{\partial^4}{\partial \theta^2 \partial z^2} + R^4\frac{\partial^4}{\partial z^4}, \qquad b_{12} = b_{21} = -\frac{\partial^3}{\partial \theta^3} - R^2\frac{\partial^3}{\partial \theta \partial z^2}, \\
b_{22} &= \frac{\partial^2}{\partial \theta^2} + \frac{R^2(1-\nu)}{2}\frac{\partial^2}{\partial z^2}, \qquad b_{13} = b_{31} = b_{23} = b_{32} = b_{33} = 0.
\end{aligned} \tag{10}$$

It is clear that $\mathcal{B}_3$ is much more involved than $\mathcal{B}_L$. This is mostly due to the higher order effects (shearing and inertia) that are implicitly incorporated in the series expansions (Boström et al., 2001; Johansson et al., 2005). There exist many other more refined classical pure bending theories, see Leissa (1973), but none of them involves so many terms; especially not the higher order time derivatives for obvious reasons. It should be stressed that $\mathcal{B}_3$ does not possess exact symmetry, just like $\mathcal{B}_6$. This is in contrast to the various bending theories given in Leissa (1973). However, contrary to $\mathcal{B}_6$, the matrix $\mathcal{B}_3$ is symmetric for $\nu = 0$ and close to symmetric for the most used values of the Poisson's ratio ν.

2.2 Shell equations in terms of u_0, v_0, w_0, v_1 and w_1

Following the procedure given in Section 2.1 the field u_1 may be eliminated by combining the equations in (6), resulting in an equation system on the form

$$\mathcal{L}_5 \vec{u}_5 = \vec{0}, \tag{11}$$

where $\vec{u}_5 = (u_0, v_0, w_0, Rv_1, Rw_1)^T$ and the operator $\mathcal{L}_5$ may be represented in line with Eq. (7). Presenting $\mathcal{L}_5$ for the η^1 expansion, the operator $\mathcal{A}_5$ may be given as

$$
\begin{aligned}
a_{11} &= 1 - \frac{1-\nu}{2}\frac{\partial^2}{\partial\theta^2} - \frac{R^2(1-\nu)}{2}\frac{\partial^2}{\partial z^2} + \frac{\rho R^2\,(1-\nu^2)}{E}\frac{\partial^2}{\partial t^2},\\
a_{22} &= -\frac{1-\nu}{2} + \frac{\partial^2}{\partial\theta^2} + \frac{R^2(1-\nu)}{2}\frac{\partial^2}{\partial z^2} - \frac{\rho R^2(1-\nu^2)}{E}\frac{\partial^2}{\partial t^2},\\
a_{33} &= \frac{1-\nu}{2}\frac{\partial^2}{\partial\theta^2} + R^2\frac{\partial^2}{\partial z^2} - \frac{\rho R^2\,(1-\nu^2)}{E}\frac{\partial^2}{\partial t^2},\\
a_{44} &= -\frac{1-\nu}{2}, \qquad a_{55} = -\frac{1-\nu}{2}\\
a_{12} &= a_{21} = \frac{3-\nu}{2}\frac{\partial}{\partial\theta}, \qquad a_{13} = a_{31} = R\nu\frac{\partial}{\partial z},\\
a_{14} &= a_{41} = -\frac{1-\nu}{2}\frac{\partial}{\partial\theta}, \qquad a_{15} = a_{51} = -\frac{R(1-\nu)}{2}\frac{\partial}{\partial z}\\
a_{23} &= a_{32} = \frac{R(1+\nu)}{2}\frac{\partial^2}{\partial\theta\partial z}, \qquad a_{24} = a_{42} = \frac{1-\nu}{2},\\
a_{25} &= a_{52} = a_{34} = a_{43} = a_{35} = a_{53} = a_{45} = a_{54} = 0.
\end{aligned}
\tag{12}
$$

Of obvious reasons, the operators $\mathcal{A}_5$ and $\mathcal{B}_5$ (not given explicitly here) are similar to $\mathcal{A}_6$ and $\mathcal{B}_6$. The chosen representation of $\mathcal{A}_5$ has been normalized so that it resembles the equations given in Leissa (1973). This result is to be compared to classical theories that involve shearing and rotary inertia, such as e.g. the theory by Naghdi and Cooper (1956) represented by $\mathcal{L}_{NC}$. Here the operator

$\mathcal{A}_{NC}$ becomes

$$
\begin{aligned}
a_{11} &= 1 - \frac{(1-\nu)\kappa^2}{2}\frac{\partial^2}{\partial\theta^2} - \frac{R^2(1-\nu)\kappa^2}{2}\frac{\partial^2}{\partial z^2} + \frac{\rho R^2\,(1-\nu^2)}{E}\frac{\partial^2}{\partial t^2},\\
a_{22} &= -\frac{(1-\nu)\kappa^2}{2} + \frac{\partial^2}{\partial\theta^2} + \frac{R^2(1-\nu)}{2}\frac{\partial^2}{\partial z^2} - \frac{\rho R^2(1-\nu^2)}{E}\frac{\partial^2}{\partial t^2},\\
a_{33} &= \frac{1-\nu}{2}\frac{\partial^2}{\partial\theta^2} + R^2\frac{\partial^2}{\partial z^2} - \frac{\rho R^2\,(1-\nu^2)}{E}\frac{\partial^2}{\partial t^2},\\
a_{44} &= -\frac{(1-\nu)\kappa^2}{2}, \qquad a_{55} = -\frac{(1-\nu)\kappa^2}{2}\\
a_{12} &= a_{21} = \frac{(3-\nu)\kappa^2}{2}\frac{\partial}{\partial\theta}, \qquad a_{13} = a_{31} = R\nu\frac{\partial}{\partial z},\\
a_{14} &= a_{41} = -\frac{(1-\nu)\kappa^2}{2}\frac{\partial}{\partial\theta}, \qquad a_{15} = a_{51} = -\frac{R(1-\nu)\kappa^2}{2}\frac{\partial}{\partial z}\\
a_{23} &= a_{32} = \frac{R(1+\nu)}{2}\frac{\partial^2}{\partial\theta\partial z}, \qquad a_{24} = a_{42} = \frac{(1-\nu)\kappa^2}{2},\\
a_{25} &= a_{52} = a_{34} = a_{43} = a_{35} = a_{53} = a_{45} = a_{54} = 0.
\end{aligned}
\tag{13}
$$

while the elements of $\mathcal{B}_{NC}$ are

$$
\begin{aligned}
b_{33} &= \frac{1-\nu}{2}\frac{\partial^2}{\partial\theta^2} \\
b_{44} &= \frac{\partial^2}{\partial\theta^2} + \frac{R^2(1-\nu)}{2}\frac{\partial^2}{\partial z^2} - \frac{\rho R^2(1-\nu^2)}{E}\frac{\partial^2}{\partial t^2}, \\
b_{55} &= \frac{1-\nu}{2}\frac{\partial^2}{\partial\theta^2} + R^2\frac{\partial^2}{\partial z^2} - \frac{\rho R^2(1-\nu^2)}{E}\frac{\partial^2}{\partial t^2}, \\
b_{14} &= b_{41} = -\frac{\partial}{\partial\theta}, \\
b_{24} &= b_{42} = -\frac{\partial^2}{\partial\theta^2} + \frac{R^2(1-\nu)}{2}\frac{\partial^2}{\partial z^2} - \frac{\rho R^2(1-\nu^2)}{E}\frac{\partial^2}{\partial t^2}, \\
b_{35} &= b_{53} = -\frac{1-\nu}{2}\frac{\partial^2}{\partial\theta^2} + R^2\frac{\partial^2}{\partial z^2} - \frac{\rho R^2(1-\nu^2)}{E}\frac{\partial^2}{\partial t^2}, \\
b_{45} &= b_{54} = \frac{R(1+\nu)}{2}\frac{\partial^2}{\partial\theta\partial z} \\
b_{11} &= b_{12} = b_{21} = b_{13} = b_{31} = b_{15} = b_{51} = b_{22} = b_{23} = b_{32} = b_{25} = b_{52} = b_{34} = b_{43} = 0.
\end{aligned}
\tag{14}
$$

The operator $\mathcal{A}_5$ is very similar to $\mathcal{A}_{NC}$ where the latter involves the shear correction factor κ^2. For $\kappa^2 = 1$ one has $\mathcal{A}_5 = \mathcal{A}_{NC}$. The shear correction factor is variously taken just less than unity (Leissa, 1973). Considering the η^1 terms, it is clear that the expansion theory $\mathcal{B}_5$ is much more involved than $\mathcal{B}_{NC}$.

3 Eigenfrequencies for a ring

Consider a 2D circular ring in plane strain vibrating in the $(r\theta)$-plane, independent of the $z-$coordinate. Hence the fields w_0 and w_1 are hereby set to zero. In this section, the eigenfrequencies for the different approximate theories are compared with each other and the exact theory. Considering a fixed frequency ω, the displacement fields may be expressed in terms of Fourier series. Each mode of $\vec{u}_6$, now consisting of only four terms, has the following representation

$$
\left.
\begin{array}{ll}
\{u_{j,0}(\omega)\mathrm{e}^{-\mathrm{i}\omega t}, & u_{j,m}(\omega)\cos m\theta\mathrm{e}^{-\mathrm{i}\omega t}\} \\
\{v_{j,0}(\omega)\mathrm{e}^{-\mathrm{i}\omega t}, & v_{j,m}(\omega)\sin m\theta\mathrm{e}^{-\mathrm{i}\omega t}\}
\end{array}
\right\} \quad j = 0, 1\ , \quad m = 1, 2 \ldots . \tag{15}
$$

The integer order of the θ-dependence results from requiring continuity of the shell fields along the tangential direction. Note that uncoupled equations are obtained for the radial displacement $u_{j,0}(\omega)$ and the tangential displacement $v_{j,0}(\omega)$. These cases correspond to purely radial and shearing modes, respectively, that are independent of θ. As the different modes m become independent of each other, they can be analyzed separately. Hence, for each

m, the nontrivial solution of $\mathcal{L}_6\vec{u}_6 = \vec{0}$ is solved numerically for ω. Note that there are $2(2j+1)$ eigenfrequencies for a fixed η^j expansion. These results are compared to the two-dimensional exact solution, where the displacement is expressed in terms of cylindrical Bessel and Neumann functions (Achenbach, 1973).

Consider the equation system (6) that is expressed in terms of the four fields u_0, v_0, u_1, v_1. Table 1 and 2 present the three lowest nondimensional eigenfrequencies $\Omega = \omega R/c_E$ where $c_E = \sqrt{E/\rho}$, for each mode $m = 0, 1, 2, 3$ when $h/R = 1/100$ and $h/R = 1/5$, respectively. Here, the exact theory is compared to series expansion theories of order η^0, η^1 and η^2. The comparisons are made in terms of the relative error. When the absolute value of the relative error is less than 10^{-7}, this is marked by a star $(*)$. These results show how the accuracy of the series solution is improved as the η^j order is increased. It is seen that the higher eigenfrequencies are not that well predicted, as expected. However, these frequencies are predicted satisfactorily by increasing the η^j order a few steps (not presented here). Moreover, the results for thin shells, $h/R = 1/100$, are superior to the ones for $h/R = 1/5$. Of course, the results from the η^0 expansion are not affected by the ratio h/R. Similar accuracies are obtained for higher order modes $m > 3$ and for frequencies $\Omega_{m,j}$ when $j > 3$.

m	Ω	Exact	η^0	η^1	η^2
$m=0$	$\Omega_{0,1}$	1.0482967	-1.14×10^{-5}	$*$	$*$
	$\Omega_{0,2}$	194.83701	–	-9.97×10^{-2}	1.38×10^{-2}
	$\Omega_{0,3}$	194.83984	–	-9.97×10^{-2}	1.38×10^{-2}
$m=1$	$\Omega_{1,1}$	0.62017626	-4.17×10^{-6}	$*$	$*$
	$\Omega_{1,2}$	1.4824781	1.38×10^{-5}	$*$	$*$
	$\Omega_{1,3}$	194.84636	–	-9.97×10^{-2}	1.38×10^{-2}
$m=2$	$\Omega_{2,1}$	0.0081195729	–	-1.87×10^{-5}	$*$
	$\Omega_{2,2}$	1.2403525	-4.17×10^{-6}	$*$	$*$
	$\Omega_{2,3}$	2.3439733	2.68×10^{-5}	$*$	$*$
$m=3$	$\Omega_{3,1}$	0.022963650	–	-3.12×10^{-5}	$*$
	$\Omega_{3,2}$	1.8605288	-4.17×10^{-6}	$*$	$*$
	$\Omega_{3,3}$	3.3148566	3.35×10^{-5}	$*$	$*$

Table 1
The eigenfrequencies for exact theory and the relative error for series expansions theories using four fields (6) of order η^0, η^1 and η^2 for $h/R = 1/100$.

Tables 3 and 4 display the corresponding results using classical membrane theory, bending theory (Love), shearing and inertia theory (Naghdi-Cooper) as well as the η^1 expansion theory using two fields u_0, v_0 according to Eq. (8). Compared to the previous results from Eq. (6), the number of eigenfrequen-

m	Ω	Exact	η^0	η^1	η^2
$m=0$	$\Omega_{0,1}$	1.0530381	-4.51×10^{-3}	-2.73×10^{-5}	-2.85×10^{-7}
	$\Omega_{0,2}$	9.7533236	–	-9.74×10^{-2}	1.34×10^{-2}
	$\Omega_{0,3}$	9.8157302	–	-9.87×10^{-2}	1.38×10^{-2}
$m=1$	$\Omega_{1,1}$	0.62119597	-1.64×10^{-3}	-1.60×10^{-5}	-1.57×10^{-7}
	$\Omega_{1,2}$	1.4740323	5.74×10^{-3}	-6.42×10^{-5}	-1.36×10^{-7}
	$\Omega_{1,3}$	9.8860272	–	-9.79×10^{-2}	1.39×10^{-2}
$m=2$	$\Omega_{2,1}$	0.15928015	–	-6.98×10^{-3}	-1.39×10^{-4}
	$\Omega_{2,2}$	1.2422917	-1.57×10^{-3}	-3.39×10^{-5}	-3.49×10^{-7}
	$\Omega_{2,3}$	2.3178905	1.13×10^{-2}	-1.91×10^{-4}	4.31×10^{-7}
$m=3$	$\Omega_{3,1}$	0.43675502	–	-1.07×10^{-2}	-2.75×10^{-4}
	$\Omega_{3,2}$	1.8631873	-1.43×10^{-3}	-6.41×10^{-5}	-7.28×10^{-7}
	$\Omega_{3,3}$	3.2676316	1.45×10^{-2}	-4.20×10^{-4}	2.60×10^{-6}

Table 2
The eigenfrequencies for exact theory and the relative error for the series expansions theories using four fields (6) of order η^0, η^1 and η^2 for $h/R = 1/5$.

cies using Eq. (8) are reduced to $2(j+1)$ for a η^j expansion. It is clear from these tables that Naghdi-Cooper and the η^1 expansion theories are superior to the membrane and Love theories, as expected. However, the Naghdi and Cooper theory renders more accurate results than the η^1 expansion theory for low frequencies. This is most likely due to the influence of the shear correction factor κ^2, which is introduced to compensate for varying thickness shear stresses for low frequencies. Note that κ^2 appears already in the lower order operator $\mathcal{A}_{NC}$. For higher frequencies the results from η^1 expansion theory are superior to the Naghdi-Cooper theory, which probably is due to the extra terms appearing in the operator $\mathcal{B}_3$. It is easy to see analytically that the higher order time derivatives become considerably more important for $\Omega > 1$. Moreover it is a bit puzzling that the membrane equation (identical to the η^0 expansion) in places gives more accurate predictions than Love's theory. However, only the theory due to Love models the important lower eigenfrequencies (especially the lowest for $m = 2$). Note that the results from the η^1 expansion using two fields u_0, v_0 (Tables 3, 4) differ somewhat from the ones using four fields u_0, v_0, u_1, v_1 (Tables 1, 2). As the results using three fields u_0, v_0, v_1 Eq. (11) only slightly deviate from the listed η^1 results, this case is not presented separately.

m	Ω	Exact	Membrane	Love	N-C	η^1
$m=0$	$\Omega_{0,1}$	1.0482967	-1.14×10^{-5}	-1.14×10^{-5}	-1.13×10^{-5}	$*$
	$\Omega_{0,2}$	194.83701	–	–	1.48×10^{-1}	-1.17×10^{-1}
	$\Omega_{0,3}$	194.83984	–	–	1.48×10^{-1}	-1.17×10^{-1}
$m=1$	$\Omega_{1,1}$	0.62017626	-4.17×10^{-6}	–	$*$	$*$
	$\Omega_{1,2}$	1.4824781	1.38×10^{-5}	1.80×10^{-5}	-6.98×10^{-6}	$*$
	$\Omega_{1,3}$	194.84636	–	–	1.48×10^{-1}	-9.15×10^{-2}
$m=2$	$\Omega_{2,1}$	0.0081195729	–	3.94×10^{-5}	2.12×10^{-6}	-2.05×10^{-5}
	$\Omega_{2,2}$	1.2403525	-4.17×10^{-6}	–	$*$	$*$
	$\Omega_{2,3}$	2.3439733	2.68×10^{-5}	3.75×10^{-5}	-2.52×10^{-6}	$*$
$m=3$	$\Omega_{3,1}$	0.022963650	–	1.22×10^{-4}	1.43×10^{-5}	-1.96×10^{-5}
	$\Omega_{3,2}$	1.8605288	-4.17×10^{-6}	–	$*$	$*$
	$\Omega_{3,3}$	3.3148566	3.35×10^{-5}	4.70×10^{-5}	2.02×10^{-6}	$*$

Table 3
The eigenfrequencies for exact theory and the relative error for membrane, Love, Naghdi-Cooper (N-C) and series expansions η^1 theories using two fields (8) for $h/R = 1/100$. N-C with $\kappa^2 = 5/6$.

4 Dispersion Relations

The performance of the 3D series expansion shell equations has been validated using the dispersion relations for waves traveling along the cylinder, parallel to the z-axis, with wavenumber k. It is noted that for $k = 0$, this yields the two-dimensional eigenfrequencies for a circular ring in plain strain as treated in the previous section. As for the 2D ring case, a fixed frequency ansatz is made and the dependency on θ is assumed to be of a Fourier series type with factors like $\sin m\theta$.

Just as in the two-dimensional case, the exact solutions are expressed in terms of cylindrical Bessel and Neumann functions (Achenbach, 1973). Note that by performing a radial series expansion of the Bessel and Neumann functions, series terms corresponding to Eq. (3) are identified. It is straightforward to show that these expressions fulfill the recursion formulas Eqs. (4). It could also be stressed here that by expanding the exact dispersion equation in power series in terms of nondimensional wavenumber kR, each term is identical to the corresponding term according to the present theory, at least for the lowest terms studied (see comparable situation for plates (Losin, 2001)).

As presented above, the shell equations have been truncated to different orders in η, and truncations including up to η^j with $j = 0, 1, 2, 3$ are plotted. There is no inherent difficulty in raising the order further, but the equations get

m	Ω	Exact	Membrane	Love	N-C	η^1
$m=0$	$\Omega_{0,1}$	1.0530381	-4.51×10^{-3}	-4.51×10^{-3}	-4.51×10^{-3}	1.99×10^{-5}
	$\Omega_{0,2}$	9.7533236	–	–	1.23×10^{-1}	-9.74×10^{-2}
	$\Omega_{0,3}$	9.8157302	–	–	1.47×10^{-1}	-9.16×10^{-2}
$m=1$	$\Omega_{1,1}$	0.62119597	-1.64×10^{-3}	–	-3.67×10^{-6}	-1.43×10^{-5}
	$\Omega_{1,2}$	1.4740323	5.74×10^{-3}	7.38×10^{-3}	-2.68×10^{-3}	1.58×10^{-5}
	$\Omega_{1,3}$	9.8860272	–	–	-1.35×10^{-1}	-9.53×10^{-2}
$m=2$	$\Omega_{2,1}$	0.15928015	–	-1.52×10^{-2}	-6.85×10^{-4}	-7.83×10^{-3}
	$\Omega_{2,2}$	1.2422917	-1.57×10^{-3}	–	1.54×10^{-5}	-3.41×10^{-5}
	$\Omega_{2,3}$	2.3178905	1.13×10^{-2}	1.56×10^{-2}	-7.04×10^{-4}	2.59×10^{-4}
$m=3$	$\Omega_{3,1}$	0.43675502	–	4.60×10^{-2}	4.80×10^{-3}	-6.66×10^{-3}
	$\Omega_{3,2}$	1.8631873	-1.43×10^{-3}	–	4.72×10^{-5}	-5.02×10^{-5}
	$\Omega_{3,3}$	3.2676316	1.45×10^{-2}	2.01×10^{-2}	1.44×10^{-3}	3.20×10^{-4}

Table 4
The eigenfrequencies for exact theory and the relative error for membrane, Love, Naghdi-Cooper (N-C) and series expansions η^1 theories using two fields (8) for $h/R = 1/5$. N-C with $\kappa^2 = 5/6$.

very involved. For validation purposes, these equations have been developed up to and including order η^4, and even higher for specific material data, but the results bring little new information: the higher the order, the better the convergence. The size of the shell equations, as stored in simplified form on a computer, grows roughly like $(j+1)^2$.

As an example of high-frequency results, exact and approximate results with terms including η^2 and η^3 have been plotted in Figure 2. Note that while the η^3 solution performs well near and far from the origin, the η^2 solutions deviate significantly from the exact solutions for the high frequencies. At the right limit of the plot, the layer thickness is twice the (rod) wavelength, indeed far beyond a "thin" layer. These results for higher frequencies just aim to show a general behavior of the theories. In some cases, the curves change path rather abruptly, giving the wrong impression that curves are crossed. Moreover, some exact solutions seem to be randomly placed. This is due to the solution procedure: the η^3 solutions are used as starting values for the search for exact solutions, and in the high frequency cases other solutions than the intended are sometimes found. However, since the main focus in the paper is the lower-frequency behavior, all these higher mode solutions have not been investigated further.

In Figures 3, 4 and 5, the dispersion curves are plotted for the thick-walled case of $h/R = 1/5$, for different $m = 0, 1$ and 2, respectively. All solutions

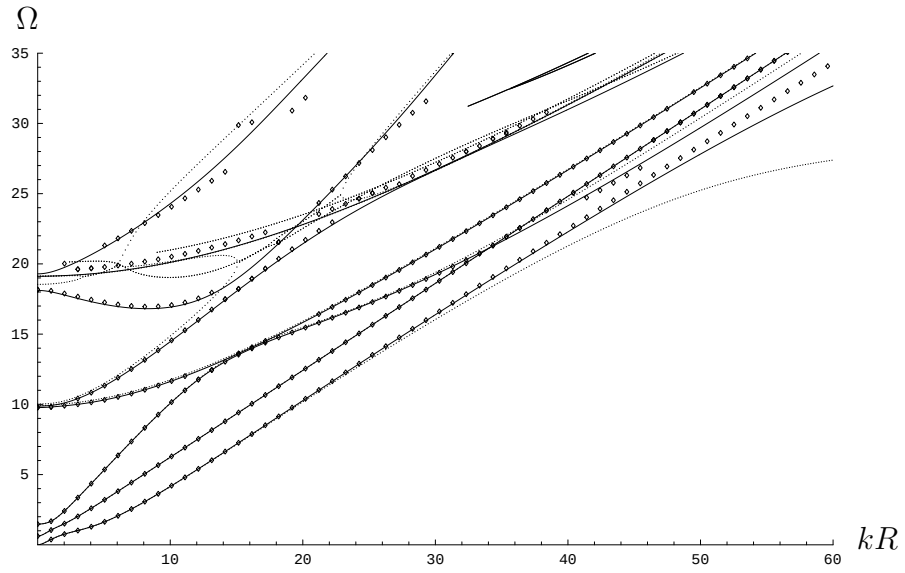

Fig. 2. Dispersion curves for modes with $m = 1$, $h/R = 1/5$, showing higher frequencies and only high approximation orders. Solid lines represent the η^3-solution, the small dots represent the η^2-solution and the rhombi represent the exact solution.

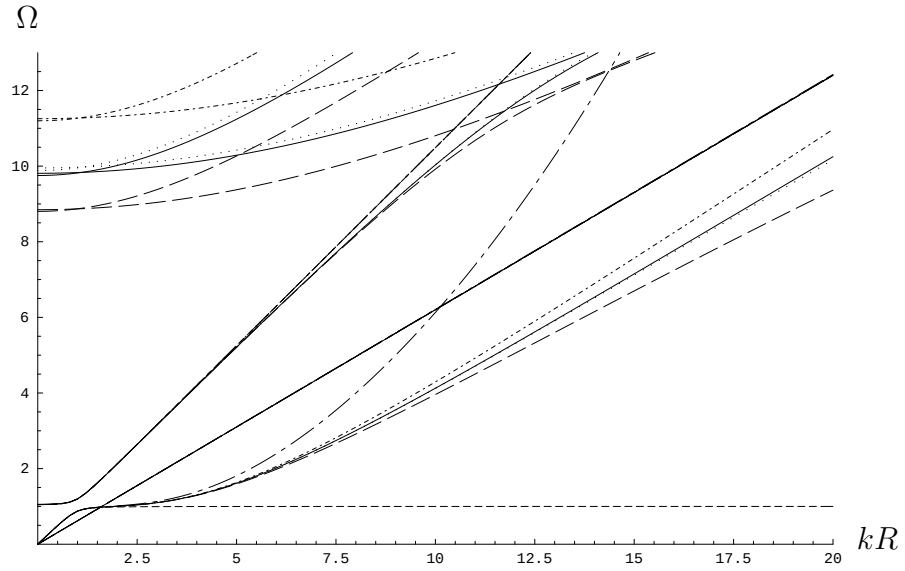

Fig. 3. Dispersion curves for modes with $m = 0$; $h/R = 1/5$. Solid lines represent the exact solution, short dashes η^0, long dashes η^1, small dots η^2, long dash-dotted Love and short dash-dotted Naghdi-Cooper.

that fit in the range shown are also plotted. The performance of the solutions with cut-off frequencies around $\Omega = 10$ is, as expected, fairly poor, and is not further commented upon.

In Figure 3, the axially symmetric case $m = 0$ is plotted. The straight lines starting from the origin represent the uncoupled torsional wave mode, accurately predicted by all theories, as expected given its dispersion-free nature. These lines cross the other curves emanating from the origin, as the latter

represent the longitudinal rod mode that are independent from the torsional mode, (Graff, 1975). Note that the η^0-solution starts off well, but shows no stiffening with raised wave numbers above approximately $kR = 1.5$. The Love solution departs visibly from the correct solution at about $kR = 3$. The η^1 and N-C solutions show similar performance, although it can be noted that while the former tends to be too soft, the latter is too stiff in this mode. The third bundle of curves to note in Figure 3, starting off at about $\Omega = 1$, represents the breathing mode. All studied solutions almost coincide up to approximately $kR = 4$, where the η^0, Love and N-C solutions together deviate visibly. The η^1 solution deviate visibly around $kR = 7$. Further uncoupled torsional mode appears in the exact case at the cutoff frequency around $\Omega = 10$, which is also represented by the higher order theories.

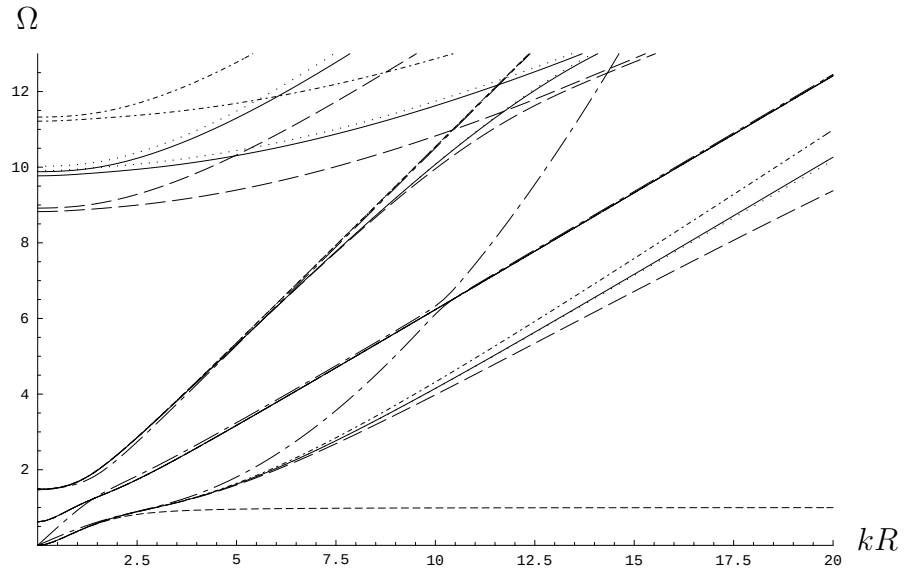

Fig. 4. Dispersion curves for modes with $m = 1$; $h/R = 1/5$. Solid lines represent the exact solution, short dashes η^0, long dashes η^1, small dots η^2, long dash-dotted Love and short dash-dotted Naghdi-Cooper.

In Figure 4, results for the case $m = 1$ are plotted. Close to the origin, different modes can be identified. For the beam-like bending mode, starting off at the origin along the horizontal axis, the Love solution fails immediately. The η^0-solution is good up to about $kR = 1.5$. As for $m = 0$, the η^1 and N-C solutions show similar performance, and follow the exact solution up to about $kR = 4$. The η^2 solution is visibly correct up to about $kR = 15$. The curves with a cut-off frequency at approximately $\Omega = 0.6$ represent a torsion-like mode. All theories except Love predicts this mode very well. The curves with a cut-off frequency at approximately $\Omega = 1.5$ represent a longitudinal mode with a shear component, since $m = 1$. Love theory fails already at about $kR = 1$. N-C and η^0 solutions deviate visibly from around $kR = 3.5$. The η^1 solution follows the exact solution until approximately $kR = 7$. Unlike the case $m = 0$, the torsion-like modes with cut-off frequencies at about $\Omega = 0.6$ and $\Omega = 10$ now couple to the other wave-types, and thus no crossing of curves occur for

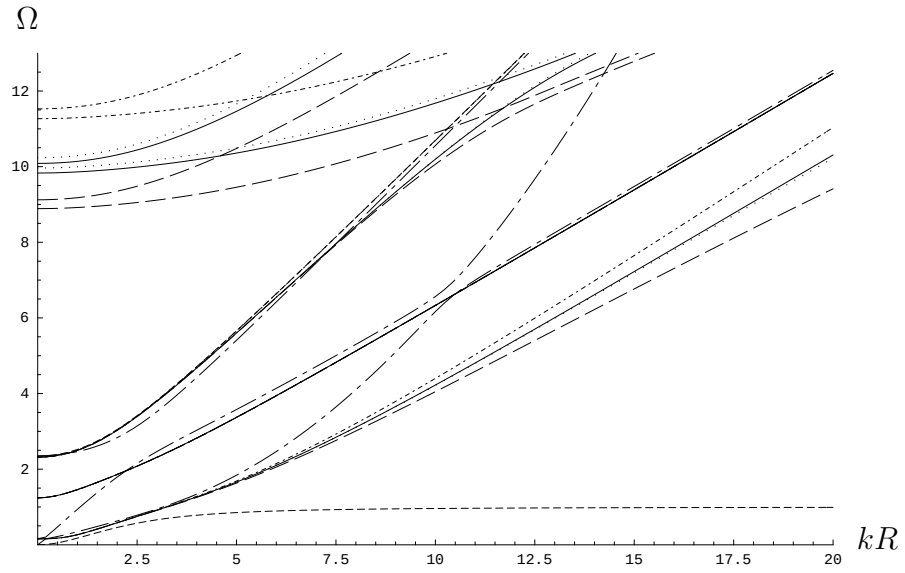

Fig. 5. Dispersion curves for modes with $m = 2$; $h/R = 1/5$. Solid lines represent the exact solution, short dashes η^0, long dashes η^1, small dots η^2, long dash-dotted Love and short dash-dotted Naghdi-Cooper.

a specific shell theory.

The curves corresponding to $m = 2$ are shown in Figure 5. Near the origin, some aspects deserve closer attention. The curves with cut-off around $\Omega = 0.2$ represent the fundamental bending mode in the circumferential direction (radial motion) of the circular cross section. The η^0 case fails to predict the cut-off frequency altogether. The Love solution deviates from the exact solution already around $kR = 0.3$. Apparently, the N-C solution departs from the exact solution at approximately $kR = 3$ as does the η^1 solution. Closer inspection reveals, however, that the latter follows much closer to the exact solution up until that point. This is generally true for the other cases where the N-C and η^1 solutions have shown similar performance levels. As for the two modes with higher cut-off frequencies, they show similar behavior as the corresponding modes for $m = 1$, and the same comments hold also for $m = 2$.

In Figure 6, the dispersion curves are plotted for the thin-walled case of $h/R = 1/100$ with $m = 0$, for the same range as in the previous plots. Close to the origin, the behavior is very similar to that shown in Figure 3 in the thick-walled case. Further away, two observations can be made: first, the performance of all theories is very good, even η^0 deviate little for wavenumbers less than $kR = 7$. Second, the variations from a straight line are pushed away from the plotted range. This indicates that it is the wall thickness h, rather than the radius of curvature R, that dictates the performance of the considered theories. Note that in all plots there is a transition region at about $\Omega = 1$ and $kR = 1$ where the dispersion curves change from being "rod-like" to "plate-like", the location of which is obviously controlled by the radius.

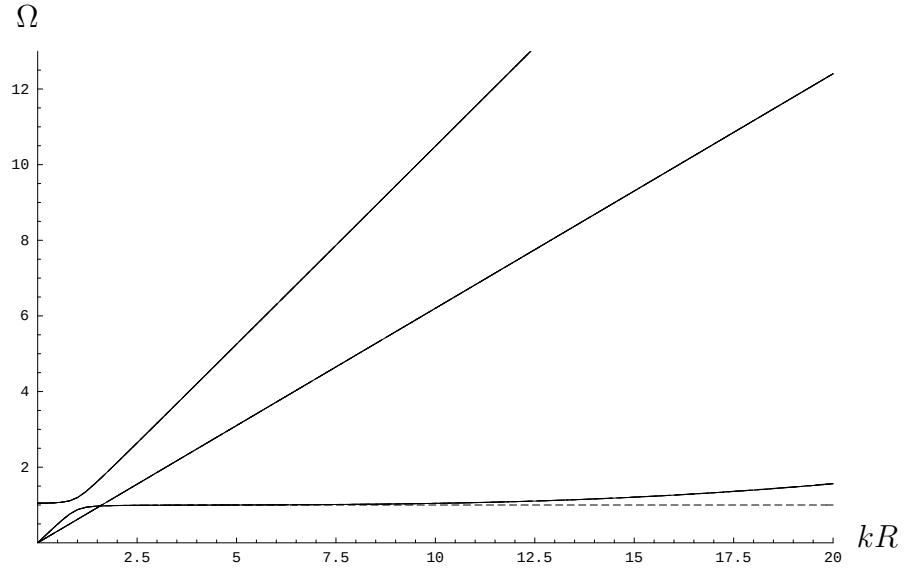

Fig. 6. Dispersion curves for modes with $m = 0$; $h/R = 1/100$. Solid lines represent the exact solution, short dashes η^0, long dashes η^1, small dots η^2, long dash-dotted Love and short dash-dotted Naghdi-Cooper.

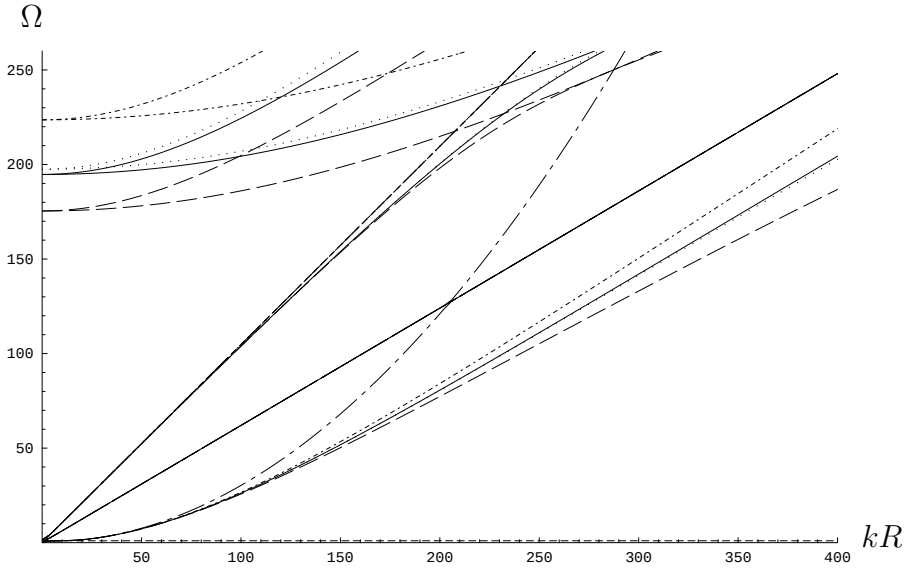

Fig. 7. Dispersion curves for modes with $m = 1$; $h/R = 1/100$. Solid lines represent the exact solution, short dashes η^0, long dashes η^1, small dots η^2, long dash-dotted Love and short dash-dotted Naghdi-Cooper.

To better compare the performance of the shell theories in the thin-walled case $h/R = 1/100$, Figure 7 presents dispersion curves for a larger range when $m = 1$. Here, the same kh-range is covered as in Figure 4 where $h/R = 1/5$. At the extreme right, these plots represent a value of $kh = 4$; in other words, the wall thickness h is $2/\pi$ times the wavelength in the axial direction. The highest frequency in the Figures 4 and 7, $\Omega = 13$ or $\Omega = 260$, corresponds to a shear wavelength that is less than double the thickness. As there is not much difference between distinct m values away from the origin, only $m = 1$

is presented here. The similarity of the higher frequencies for different values of h/R or different m is striking when comparing Figure 3, 4, 5 and Figure 7.

5 Concluding remarks

This paper considers derivation of dynamical cylindrical shell equations. Using a series expansion technique in the radial coordinate, a set of partial differential equations are obtained that are believed to be asymptotically correct. The set of equations are expressed in terms of six, five and three fields, respectively. The explicit representation is given up to order η^1 corresponding to thickness order h^2. Considering the representations using five or three fields, these expressions are compared analytically to classical shell equations. Numerical results give the dispersion curves and the 2D lowest eigenfrequencies for different circumferential orders. Here, the expansion theory is compared to exact theory as well as classical theories. In all cases, the expansion theory renders satisfying results. f

For the future there are good reasons to believe that the series expansion techniques can be successfully applied to similar more complicated problems, e.g. anisotropic and layered cylindrical shells or doubly curved surfaces. Such structures have large strength to weight ratio, which is of utmost importance in engineering. However, new materials and modern high performance constructions put great demands on the engineers modeling abilities. This calls for more accurate tools to model advanced shells properly. There is a wealth of more or less systematically developed shell theories in the literature, based on simplifying kinematics. For more complicated structures, the status of such simplifications are partially unclear. Hence, there are needs to develop new equations in a rigorous way, in line with what is presented in this paper.

What has not been presented in the current paper is how to implement the derived equations in a bounded case, including edge boundary conditions. Such higher order end boundary conditions can be derived in an equally systematic manner using variational methods, previously adopted for homogeneous rods (Mauritsson and Folkow, 2008). Eventually, the new shell equations may be implemented in a FE environment, where shell elements still are preferable to 3D elements due to reasonable length-to-thickness ratio of the elements.

Appendix A

Consider Eq. (6) where the matrix operator is truncated as $\mathcal{L}_6 = \mathcal{A}_6 + \eta\mathcal{B}_6$. Below is the explicit representation of the matrix elements, written in terms

of the modulus of elasticity E and Poissons ratio ν. Here, the equations are normalized in consequence with the representations in Section 2.1 and Section 2.2. It should be mentioned that the last row is actually obtained through a linear combination of $\Delta\sigma_{rz} = 0$ and $\Sigma\sigma_{rz} = 0$ in order to make $\mathcal{A}_6$ symmetric. The operator $\mathcal{B}_6$ is seen to be rather complicated, involving fourth order differentiations. Moreover, it is not symmetric, even though several terms are indicating an almost symmetric pattern.

The 36 elements of $\mathcal{A}_6$ ar

$$
\begin{aligned}
a_{11} &= \frac{(1-\nu)^2}{(1-2\nu)} - \frac{1-\nu}{2}\frac{\partial^2}{\partial\theta^2} - \frac{R^2(1-\nu)}{2}\frac{\partial^2}{\partial z^2} + \frac{\rho R^2(1-\nu^2)}{E}\frac{\partial^2}{\partial t^2},\\
a_{22} &= -\frac{1-\nu}{2} + \frac{(1-\nu)^2}{(1-2\nu)}\frac{\partial^2}{\partial\theta^2} + \frac{R^2(1-\nu)}{2}\frac{\partial^2}{\partial z^2} - \frac{\rho R^2(1-\nu^2)}{E}\frac{\partial^2}{\partial t^2},\\
a_{33} &= \frac{1-\nu}{2}\frac{\partial^2}{\partial\theta^2} + \frac{R^2(1-\nu)^2}{(1-2\nu)}\frac{\partial^2}{\partial z^2} - \frac{\rho R^2(1-\nu^2)}{E}\frac{\partial^2}{\partial t^2},\\
a_{44} &= \frac{(1-\nu)^2}{1-2\nu}, \qquad a_{55} = -\frac{1-\nu}{2} \qquad a_{66} = -\frac{1-\nu}{2},\\
a_{12} &= a_{21} = \frac{(1-\nu)(3-4\nu)}{2(1-2\nu)}\frac{\partial}{\partial\theta}, \qquad a_{13} = a_{31} = \frac{R\nu(1-\nu)}{1-2\nu}\frac{\partial}{\partial z},\\
a_{14} &= a_{41} = \frac{\nu(1-\nu)}{1-2\nu} \qquad a_{15} = a_{51} = -\frac{1-\nu}{2}\frac{\partial}{\partial\theta}, \qquad a_{16} = a_{61} = -\frac{R(1-\nu)}{2}\frac{\partial}{\partial z},\\
a_{23} &= a_{32} = \frac{R(1-\nu)}{2(1-2\nu)}\frac{\partial^2}{\partial\theta\partial z}, \qquad a_{24} = a_{42} = \frac{\nu(1-\nu)}{1-2\nu}\frac{\partial}{\partial\theta} \qquad a_{25} = a_{52} = \frac{1-\nu}{2},\\
a_{34} &= a_{43} = \frac{\nu(1-\nu)}{1-2\nu}\frac{\partial}{\partial z},\\
a_{26} &= a_{62} = a_{35} = a_{53} = a_{36} = a_{63} = a_{45} = a_{54} = a_{46} = a_{64} = a_{56} = a_{65} = 0.
\end{aligned}
$$

The elements of $\mathcal{B}_6$ are:

$$b_{11} = \frac{3(1-\nu)}{2} - \frac{21-53\nu+34\nu^2}{4(1-2\nu)}\frac{\partial^2}{\partial\theta^2} - \frac{R^2(1-5\nu+6\nu^2)}{4(1-2\nu)}\frac{\partial^2}{\partial z^2} + \frac{\rho R^2(1+\nu)(2-3\nu)}{2E}\frac{\partial^2}{\partial t^2}$$
$$- \frac{\nu}{4}\frac{\partial^4}{\partial\theta^4} - \frac{R^2\nu}{2}\frac{\partial^4}{\partial\theta^2\partial z^2} - \frac{\rho R^2(1+\nu)(1-4\nu)}{4E}\frac{\partial^4}{\partial\theta^2\partial t^2} - \frac{\rho R^4(1+\nu)(1-4\nu)}{4E}\frac{\partial^4}{\partial z^2\partial t^2} - \frac{R^4\nu}{4}\frac{\partial^4}{\partial z^4},$$
$$+ \frac{\rho^2R^4(1+\nu)^2(1-2\nu)}{2E^2}\frac{\partial^4}{\partial t^4},$$
$$b_{12} = \frac{15-17\nu}{4}\frac{\partial}{\partial\theta} - \frac{12-25\nu+14\nu^2}{4(1-2\nu)}\frac{\partial^3}{\partial\theta^3} - \frac{R^2(4-5\nu)}{4}\frac{\partial^3}{\partial\theta\partial z^2} + \frac{\rho R^2(1+\nu)(11-10\nu)}{4E}\frac{\partial^3}{\partial\theta\partial t^2},$$
$$b_{13} = -\frac{3R(1-\nu)}{2(1-2\nu)}\frac{\partial^3}{\partial\theta^2\partial z} + \frac{R^3(1-\nu)}{2}\frac{\partial^3}{\partial z^3} - \frac{\rho R^3(1+\nu)}{2E}\frac{\partial^3}{\partial z\partial t^2},$$
$$b_{14} = -\frac{3(1-\nu)}{2} - \frac{3\nu(1-\nu)}{1-2\nu}\frac{\partial^2}{\partial\theta^2} + \frac{\rho R^2(1+\nu)}{2E}\frac{\partial^2}{\partial t^2},$$
$$b_{15} = -\frac{13-11\nu}{4}\frac{\partial}{\partial\theta} + \frac{2-\nu}{4}\frac{\partial^3}{\partial\theta^3} + \frac{R^2(2-\nu)}{4}\frac{\partial^3}{\partial\theta\partial z^2} - \frac{\rho R^2(1+\nu)(3-2\nu)}{4E}\frac{\partial^3}{\partial\theta\partial t^2},$$
$$b_{16} = -\frac{R(1+\nu)}{4}\frac{\partial}{\partial z} + \frac{R^3(2-\nu)}{4}\frac{\partial^3}{\partial z^3} + \frac{R(2-\nu)}{4}\frac{\partial^3}{\partial\theta^2\partial z} - \frac{\rho R^3(1+\nu)(3-2\nu)}{4E}\frac{\partial^3}{\partial z\partial t^2},$$

$$b_{21} = \frac{(1-\nu)(10-17\nu)}{2(1-2\nu)}\frac{\partial}{\partial\theta} - \frac{7-18\nu+14\nu^2}{4(1-2\nu)}\frac{\partial^3}{\partial\theta^3} - \frac{R^2(5-12\nu+10\nu^2)}{4(1-2\nu)}\frac{\partial^3}{\partial\theta\partial z^2}$$
$$+ \frac{\rho R^2(1+\nu)(2-6\nu+5\nu^2)}{E(1-2\nu)}\frac{\partial^3}{\partial\theta\partial t^2},$$
$$b_{22} = -\frac{3(1-\nu)}{2} + \frac{17-48\nu+34\nu^2}{4(1-2\nu)}\frac{\partial^2}{\partial\theta^2} - \frac{3\rho R^2(1-\nu^2)}{2E}\frac{\partial^2}{\partial t^2} - \frac{(1-\nu)(2-\nu)}{2(1-2\nu)}\frac{\partial^4}{\partial\theta^4}$$
$$+ \frac{\rho R^2(1+\nu)(4-9\nu+4\nu^2)}{2E(1-2\nu)}\frac{\partial^4}{\partial\theta^2\partial t^2} - \frac{R^4(1-\nu)}{4}\frac{\partial^4}{\partial z^4} + \frac{3R^2(1-\nu)}{4}\frac{\partial^2}{\partial z^2}$$
$$- \frac{R^2(1-\nu)(5-4\nu)}{4(1-2\nu)}\frac{\partial^4}{\partial\theta^2\partial z^2} + \frac{\rho R^4(1-\nu^2)}{E}\frac{\partial^4}{\partial z^2\partial t^2} - \frac{\rho^2R^4(1+\nu)^2(1-\nu)}{E^2}\frac{\partial^4}{\partial t^4},$$
$$b_{23} = \frac{3R(1-\nu)}{4(1-2\nu)}\frac{\partial^2}{\partial\theta\partial z} - \frac{3R(1-\nu)}{4(1-2\nu)}\frac{\partial^4}{\partial\theta^3\partial z} - \frac{3R^3(1-\nu)}{4(1-2\nu)}\frac{\partial^4}{\partial\theta\partial z^3} + \frac{\rho R^3(1+\nu)(2-3\nu)}{2E(1-2\nu)}\frac{\partial^4}{\partial\theta\partial z\partial t^2},$$
$$b_{24} = -\frac{(1-\nu)(4-11\nu)}{2(1-2\nu)}\frac{\partial}{\partial\theta} - \frac{1-\nu^2}{2(1-2\nu)}\frac{\partial^3}{\partial\theta^3} - \frac{R^2(1-\nu^2)}{2(1-2\nu)}\frac{\partial^3}{\partial\theta\partial z^2} + \frac{\rho R^2(1+\nu)(1-2\nu^2)}{2E(1-2\nu)}\frac{\partial^3}{\partial\theta\partial t^2},$$
$$b_{25} = \frac{3(1-\nu)}{2} - \frac{3(3-2\nu)}{4}\frac{\partial^2}{\partial\theta^2},$$
$$b_{26} = -\frac{3R}{4}\frac{\partial^2}{\partial\theta\partial z},$$

$$b_{31} = -\frac{R(4-5\nu)}{4(1-2\nu)}\frac{\partial^3}{\partial\theta^2\partial z} - \frac{R^3(2+\nu-4\nu^2)}{4(1-2\nu)}\frac{\partial^3}{\partial z^3} + \frac{\rho R^3(1+\nu)(1+\nu-4\nu^2)}{2E(1-2\nu)}\frac{\partial^3}{\partial z\partial t^2},$$
$$b_{32} = \frac{R}{4}\frac{\partial^2}{\partial\theta\partial z} - \frac{3R(1-\nu)}{4(1-2\nu)}\frac{\partial^4}{\partial\theta^3\partial z} - \frac{3R^3(1-\nu)}{4(1-2\nu)}\frac{\partial^4}{\partial\theta\partial z^3} + \frac{\rho R^3(1+\nu)(2-3\nu)}{2E(1-2\nu)}\frac{\partial^4}{\partial\theta\partial z\partial t^2},$$
$$b_{33} = \frac{(1-\nu)}{2}\frac{\partial^2}{\partial\theta^2} - \frac{(1-\nu)}{4}\frac{\partial^4}{\partial\theta^4} - \frac{R^2(1-\nu)(5-4\nu)}{4(1-2\nu)}\frac{\partial^4}{\partial\theta^2\partial z^2} + \frac{\rho R^2(1-\nu^2)}{E}\frac{\partial^4}{\partial\theta^2\partial t^2}$$
$$+ \frac{\rho R^4(1+\nu)(4-9\nu+4\nu^2)}{2E(1-2\nu)}\frac{\partial^4}{\partial z^2\partial t^2} - \frac{R^4(1-\nu)(2-\nu)}{2(1-2\nu)}\frac{\partial^4}{\partial z^4}, -\frac{\rho^2R^4(1-\nu^2)}{E^2}\frac{\partial^4}{\partial t^4},$$
$$b_{34} = -\frac{R(1-\nu^2)}{2(1-2\nu)}\frac{\partial^3}{\partial\theta^2\partial z} - \frac{R^3(1-\nu^2)}{2(1-2\nu)}\frac{\partial^3}{\partial z^3} + \frac{\rho R^3(1+\nu)(1-2\nu^2)}{2E(1-2\nu)}\frac{\partial^3}{\partial z\partial t^2},$$
$$b_{35} = -\frac{R(1-2\nu)}{4}\frac{\partial^2}{\partial\theta\partial z},$$
$$b_{36} = -\frac{3(1-\nu)}{4}\frac{\partial^2}{\partial\theta^2} + \frac{R^2(2-\nu)}{4}\frac{\partial^2}{\partial z^2} - \frac{\rho R^2(1-\nu^2)}{2E}\frac{\partial^2}{\partial t^2},$$

$$b_{41} = -\frac{3(1-\nu)}{2} + \frac{3(4-11\nu+8\nu^2)}{4(1-2\nu)}\frac{\partial^2}{\partial\theta^2} + \frac{3\rho R^2(1+\nu)}{2E}\frac{\partial^2}{\partial t^2} + \frac{3R^2\nu}{4(1-2\nu)}\frac{\partial^2}{\partial z^2},$$
$$b_{42} = -\frac{3(4-5\nu)}{4}\frac{\partial}{\partial\theta} + \frac{3(1-\nu)^2}{2(1-2\nu)}\frac{\partial^3}{\partial\theta^3} + \frac{3R^2(1-\nu)^2}{2(1-2\nu)}\frac{\partial^3}{\partial\theta\partial z^2} - \frac{3\rho R^2(1-\nu^2)}{2E}\frac{\partial^3}{\partial\theta\partial t^2},$$
$$b_{43} = \frac{3R(1-\nu)^2}{2(1-2\nu)}\frac{\partial^3}{\partial\theta^2\partial z} + \frac{3R^3(1-\nu)^2}{2(1-2\nu)}\frac{\partial^3}{\partial z^3} - \frac{3\rho R^3(1-\nu^2)}{2E}\frac{\partial^3}{\partial z\partial t^2},$$
$$b_{44} = \frac{3(1-\nu)}{2} + \frac{3\nu(1-\nu)}{2(1-2\nu)}\frac{\partial^2}{\partial\theta^2} + \frac{3R^2\nu(1-\nu)}{2(1-2\nu)}\frac{\partial^2}{\partial z^2} + \frac{3\rho R^2(1-\nu^2)}{2E}\frac{\partial^2}{\partial t^2},$$
$$b_{45} = \frac{3(4-3\nu)}{4}\frac{\partial}{\partial\theta}$$
$$b_{46} = \frac{3R\nu}{4}\frac{\partial}{\partial z},$$

$$
\begin{aligned}
b_{51} &= -\frac{3(1-\nu)(3-5\nu)}{2(1-2\nu)}\frac{\partial}{\partial\theta} + \frac{3\nu}{4}\frac{\partial^3}{\partial\theta^3} + \frac{3R^2\nu}{4}\frac{\partial^3}{\partial\theta\partial z^2} - \frac{3\rho R^2\nu(1+\nu)}{2E}\frac{\partial^3}{\partial\theta\partial t^2},\\
b_{52} &= \frac{3(1-\nu)}{2} - \frac{3(4-11\nu+8\nu^2)}{4(1-2\nu)}\frac{\partial^2}{\partial\theta^2},\\
b_{53} &= \frac{3R(1-\nu)}{4(1-2\nu)}\frac{\partial^2}{\partial\theta\partial z},\\
b_{54} &= \frac{3(1-\nu)(1-3\nu)}{2(1-2\nu)}\frac{\partial}{\partial\theta},\\
b_{55} &= \frac{3(1-\nu)}{2} - \frac{3(2-\nu)}{4}\frac{\partial^2}{\partial\theta^2} - \frac{3R^2(1-\nu)}{4}\frac{\partial^2}{\partial z^2} + \frac{3\rho R^2(1-\nu^2)}{2E}\frac{\partial^2}{\partial t^2},\\
b_{56} &= -\frac{3R}{4}\frac{\partial^2}{\partial\theta\partial z},
\end{aligned}
$$

$$
\begin{aligned}
b_{61} &= -\frac{3R(1-\nu)^2}{2(1-2\nu)}\frac{\partial}{\partial z} - \frac{3R}{4}\frac{\partial^3}{\partial\theta^2\partial z} - \frac{3R^3\nu}{4}\frac{\partial^3}{\partial z^3} + \frac{3\rho R^3\nu(1+\nu)}{2E}\frac{\partial^3}{\partial z\partial t^2},\\
b_{62} &= -\frac{3R(2-5\nu+4\nu^2)}{4(1-2\nu)}\frac{\partial^2}{\partial\theta\partial z},\\
b_{63} &= -\frac{9(1-\nu)}{4}\frac{\partial^2}{\partial\theta^2} - \frac{3R^2(1-\nu)^2}{2(1-2\nu)}\frac{\partial^2}{\partial z^2} + \frac{3\rho R^2(1-\nu^2)}{2E}\frac{\partial^2}{\partial t^2},\\
b_{64} &= -\frac{3R\nu(1-\nu)}{2(1-2\nu)}\frac{\partial}{\partial z},\\
b_{65} &= \frac{3R}{4}\frac{\partial^2}{\partial\theta\partial z},\\
b_{66} &= -\frac{3(1-\nu)}{2} + \frac{3(1-\nu)}{4}\frac{\partial^2}{\partial\theta^2} + \frac{3R^2(2-\nu)}{4}\frac{\partial^2}{\partial z^2} - \frac{3\rho R^2(1-\nu^2)}{2E}\frac{\partial^2}{\partial t^2},
\end{aligned}
$$

References

Achenbach, J.D., 1973. *Wave Propagation in Elastic Solids*. North-Holland, Amsterdam.

Armenakas, A.E., Gazis, D.C., Herrmann, G., 1969. *Free vibrations of circular cylindrical shells*. Pergamon Press, New York.

Boström, A., 2000. On wave equations for elastic rods. *Z. Angew. Math. Mech.*, 80:245–251.

Boström, A., Johansson, G., Olsson, P., 2001. On the rational derivation of a hierarchy of dynamic equations for a homogeneous, isotropic, elastic plate. *Int. J. Solids Struct.*, 38:2487–2501.

Faraji, S., Archer, R.R., 1985. Method of initial functions for thick shells. *Int. J. Solids Struct.*, 21:851–863.

Gardner, T.G., 1985. Vibration of shear deformable rings: Theory and experiment. *J. Sound Vib.*, 103:549–565.

Gazis, D.C., 1958. Exact analysis of the plane-strain vibrations of thick-walled hollow cylinders. *J. Acoust. Soc. Am.*, 30:786–794.

Graff, K.F., 1975. *Wave Motion in Elastic Solids*. Clarendon Press, Oxford.

Hirano, K., Hirashima, K., 1989. Formulation and accuracy of the circular cylindrical shell theory due to higher order approximation. *JSME Int. J., Series I*, 32:337–340.

Johansson, G., Niklasson, A.J., 2003. Approximate dynamic boundary conditions for a thin piezoelectric layer. *Int. J. Solids Struct.*, 40:3477–3492.

Johansson, M., Folkow, P.D., 2007. Approximate boundary conditions for thin porous layers *To be submitted for publication.*

Johansson, M., Folkow, P.D., Hägglund, A.M., Olsson, P., 2005. Approximate boundary conditions for a fluid-loaded elastic plate. *J. Acoust. Soc. Am.*, 118:3436–3446.

Johnson, M.W., Widera, O.E., 1969. An asymptotic dynamic theory for cylindrical shells. *Stud. appl. Math.*, 48:205–226.

Kennard, E.H., 1953. The new approach to shell theory: Circular cylinders. *J. Appl. Mech.*, 20:33–40.

Leissa, A.W., 1973. *Vibration of Shells*. NASA SP-288, Washington DC: US Government Printing Office.

Losin, N.A., 1997. Asymptotics of flexural waves in isotropic elastic plates. *J. Appl. Mech.*, 64:336–342.

Losin, N.A., 1998. Asymptotics of extensional waves in isotropic elastic plates. *J. Appl. Mech.*, 65:1042–1047.

Losin, N.A., 2001. On the equivalence of dispersion relations resulting from Rayleigh-Lamb frequency equation and the operator plate model. *J. Vibr. Acoust.*, 123:417–420.

McDaniel, J.G., Ginsberg, J.H., 1993. Thickness expansions for higher-order effects in vibrating cylindrical shells. *J. Appl. Mech.*, 60:463–469.

McNiven, H.D., Shah, A.H., Sackman, J.L., 1966. Axially symmetric waves in hollow, elastic rods: Part I. *J. Acoust. Soc. Am.*, 40:784–792.

Mauritsson, K., Boström, A., Folkow, P.D., 2008. Modelling of thin piezoelectric layers on plates. *Accepted for publication in Wave Motion.*

Mauritsson, K., Folkow, P.D., 2008. Boundary conditions for higher order rod theories. *Submitted for publication.*

Mirsky, I., Herrmann, G., 1957. Nonaxially symmetric motions of cylindrical shells. *J. Acoust. Soc. Am.*, 29:1116–1123.

Naghdi, P.M., 1956. A survey of recent progress in the theory of elastic shells. *Appl. Mech. Rev.*, 9:365–368.

Naghdi, P.M., Berry, J.G., 1954. On the equations of motion of cylindrical shells. *J. Appl. Mech.*, 21:160–166.

Naghdi, P.M., Cooper, R.M., 1956. Propagation of elastic waves in cylindrical shells, including the effects of transverse shear and rotatory inertia. *J. Acoust. Soc. Am.*, 28:56–63.

Niordson, F.I., 2000. An asymptotic theory for circular cylindrical shells. *Int. J. Solids Struct.*, 37:1817–1839.

Qatu, M.S., 2002. Recent research advances in the dynamic behavior of shells: 1989-2000, part 2: Homogeneous shells. *Appl. Mech. Rev.*, 55:415–434.

Sanders, J.L., 1959. An improved first approximation theory for thin shells. *NASA TR-R24*.

Soedel, W., 1982. On the vibration of shells with Timoshenko-Mindlin type shear deflections and rotatory inertia. *J. Sound Vib.*, 83:67–79.